

Evaluating and improving the cluster variation method entropy functional for Ising alloys

Luiz G. Ferreira^{(a),(b)}, C. Wolverton^(a), and Alex Zunger^(a)

^(a)National Renewable Energy Laboratory, Golden, CO 80401

^(b)Instituto de Física, Universidade Estadual de Campinas, 13083-970 Campinas, São Paulo, Brazil
(August 10, 2018)

The success of the “Cluster Variation Method” (CVM) in reproducing quite accurately the free energies of Monte Carlo (MC) calculations on Ising models is explained in terms of identifying a cancellation of errors: We show that the CVM produces correlation functions that are too close to zero, which leads to an *overestimation* of the exact energy, E , and at the same time, to an *underestimation* of $-TS$, so the free energy $F = E - TS$ is more accurate than either of its parts. This insight explains a problem with “hybrid methods” using MC correlation functions in the CVM entropy expression: They give exact energies E and do not give significantly improved $-TS$ relative to CVM, so they do not benefit from the above noted cancellation of errors. Additionally, “hybrid methods” suffer from the difficulty of adequately accounting for both ordered and disordered phases in a consistent way. A different technique, the “Entropic Monte Carlo” (EMC), is shown here to provide a means for critically evaluating the CVM entropy. Inspired by EMC results, we find a universal and simple correction to the CVM entropy which produces individual components of the free energy with MC accuracy, but is computationally much less expensive than either MC thermodynamic integration or EMC.

PACS numbers: 64.60.C, 05.50.+q

I. INTRODUCTION

The physics of phase transitions and phase stability of alloys is often couched in terms of statistical mechanics models on the generalized (long-range pair and multi-body interactions) Ising lattice and computed most accurately with Monte Carlo (MC) methods¹. These are time consuming calculations and usually are thus restricted to coarse grids of chemical potential and temperatures. Further, MC simulations do not give directly the values of important thermodynamic variables such as entropy and free energy, since these quantities cannot be written in terms of ensemble averages. Instead, these are obtained laboriously by integration of thermodynamic relations from a known starting point. To remedy this situation, one often uses the less accurate Molecular Field methods, most notably the Cluster Variation Method (CVM) of Kikuchi². Despite its great simplicity, the CVM reproduces many of the features of phase diagrams obtained by the many-orders-of-magnitude more computer expensive MC method: For the fcc nearest-neighbor antiferromagnetic Ising Hamiltonian with coupling constant J and zero chemical field $h=0$, the transition temperature T_c ³ from MC simulations is 1.74⁴ while CVM in the Tetrahedron (Tetrahedron-Octahedron) approximation gives 1.89 (1.81). This and other successes of the CVM² are even more surprising in light of the finding that the CVM correlation functions (the thermal average of products of the Ising spin variables) differ considerably from the exact MC values: For example, in the nearest-neighbor fcc antiferromagnetic Ising model, the MC pair correlation functions⁵ at $T = 1.9$

and $h = 0$ are -0.208 , 0.254 , 0.036 , 0.076 for the first to fourth neighbors, respectively, while the tetrahedron-CVM first neighbor correlation function is -0.188 and the tetrahedron-octahedron-CVM first and second neighbor correlation functions are -0.198 and $+0.198$. Thus, CVM correlation functions are substantially closer to zero (i.e., more “random”) than the exact values. The error in tetrahedron-CVM first neighbor correlation function leads to a $\sim 10\%$ error in both energy and entropy relative to MC (see below). However, despite such systematic discrepancies (of $\sim 10\%$ or less) in reproducing correlation functions, the CVM seems to describe well thermodynamic properties (e.g., free energies) which depend on these very correlation functions. The subject of this paper is precisely these types of errors in CVM energy, entropy, and free energy relative to MC. We make four points:

(i) We show that a reason for the success of the CVM in describing the *free energy* is an interesting cancellation of errors: The closer-to-zero CVM correlation functions imply greater randomness and hence an *overestimation* of the internal energy compared to MC. However, the more random CVM correlations also lead to a larger entropy, and hence to an *underestimation* of the $-TS$ term. Thus, the error in internal energy is of opposite sign to the error in the $-TS$ term, so these two errors partially cancel in the free energy. This cancellation of errors is due to the fact that the CVM free energy expression may be obtained from a variational argument,² but not E or S individually.

(ii) Our analysis gives insight into the successes and failures of various approaches that attempt to improve

CVM by “borrowing” certain quantities from MC. Indeed, for some applications, one may require accuracies and flexibilities beyond those provided by the CVM, and so there is a desire in the field to find accurate “hybrid” methods combining the simplicity of the CVM with the accuracy and flexibility of MC. A natural possibility is to use⁶ the correlation functions Π_{MC} (or cluster probabilities) obtained from MC simulations in the CVM expression for free energy $F_{\text{CVM}}(\Pi_{\text{MC}})$ in the hope of obtaining a more accurate free energy. We demonstrate that these methods⁶ are unlikely to succeed, as these approximations do not benefit from the cancellations of errors noted above.

(iii) We use the “Entropic Monte Carlo” (EMC) method of Lee,⁷ which provides a method for determining the entropy as a function of any state variable. We apply EMC to the case of the CVM entropy as the state variable, and demonstrate that $S_{\text{EMC}}(S_{\text{CVM}})$ provides a means for critically evaluating the errors in CVM entropy. The calculation of $S_{\text{EMC}}[S_{\text{CVM}}(\Pi_{\text{MC}})]$ further shows that this functional accurately describes $S_{\text{MC}}(\Pi_{\text{MC}})$ and thus the Monte Carlo free energy. However, this approach is computationally intensive. Finally, inspired by the EMC philosophy,

(iv) We develop a functional $\tilde{S}[S_{\text{CVM}}(\Pi_{\text{MC}})]$ that reproduces the exact $S_{\text{MC}}(\Pi_{\text{MC}})$ very closely, and is computationally much less expensive than either MC thermodynamic integration or EMC. This functional permits one to borrow from MC calculations the correlation functions (or cluster probabilities), evaluate the ensuing CVM entropy $S_{\text{CVM}}(\Pi_{\text{MC}})$, and thus obtain the nearly exact entropy $\tilde{S}[S_{\text{CVM}}(\Pi_{\text{MC}})] \approx S_{\text{MC}}(\Pi_{\text{MC}})$ and energy $E(\Pi_{\text{MC}})$. This approach thus combines the accuracy of MC with the computational simplicity of the CVM.

II. METHODS

All of the calculations described in this paper will be tests of the various methods on the fcc nearest-neighbor antiferromagnetic Ising model.

A. CVM Quantities

We first briefly review our notation. Let σ mean a configuration (“microstate”) of Ising spins (± 1) on a lattice. Consider a cluster (“figure”) f with k_f lattice points. The spin variable, which takes on the value $\hat{S}_i(\sigma) = -1(+1)$ if there is an A (B) atom at site i of the figure, depends on the configuration σ of spins in the lattice. Consider now all the clusters Rf obtained from the cluster f by the symmetry operations R of the space group of the lattice. In the CVM, we define the correlation function $\bar{\Pi}_f(\sigma)$ for the cluster f in the configuration σ as the product of spin variables over the sites of f , averaged over all the figures obtained from f by the space group operations R :

$$\bar{\Pi}_f(\sigma) = \frac{\sum_R \hat{S}_1 \hat{S}_2 \dots \hat{S}_{k_f}}{\sum_R 1}. \quad (1)$$

The CVM treats the correlation functions $\{\bar{\Pi}_f\}$ as thermodynamic variables. For a cluster f of k_f sites there are 2^{k_f} arrangements of spins ± 1 at its sites. Each arrangement j has a cluster probability ρ_j^f which is linearly dependent on the correlation function values for all subclusters of f . The correlation functions $\{\bar{\Pi}_f\}$ (or equivalently, cluster probabilities) are determined by minimizing the free energy, composed of the CVM internal energy

$$E_{\text{CVM}} = \sum_{f \subseteq F} D_f J_f \langle \bar{\Pi}_f \rangle \quad (2)$$

and the CVM entropy

$$S_{\text{CVM}} = -k \sum_{f \subseteq F} B^f \sum_j \rho_j^f \ln(\rho_j^f) \quad (3)$$

both written as a sum over all the subclusters of the maximum F . In the CVM entropy expression, one also sums over the arrangements of spins at the sites of each subcluster. The Barker coefficients B^f can be obtained from purely group theoretical arguments.^{8,9} Unless otherwise noted, all CVM calculations described in this paper are for the fcc tetrahedron approximation.

In order to examine the errors involved in the CVM, we first compute the accurate energy, entropy, and free energy from Monte Carlo simulations of the nearest-neighbor anti-ferromagnetic Ising model at $h=0$.

B. Monte Carlo Quantities

A Monte Carlo cell of 1728 sites was used with 10^6 Monte Carlo steps per site at each temperature. Although finite-size effects were not taken into account, the calculated heat capacity showed a sharp peak at $T = 1.77$, within $\sim 1\text{-}2\%$ of the most precise values for the transition temperature given in the literature $\sim 1.74\text{-}1.75$.⁴ The energy is given directly from MC, while the entropy is obtained by thermodynamic integration down from infinite temperature:

$$S(T) = k \ln 2 + \frac{E(T)}{T} - \int_0^{\frac{1}{T}} E(T) d(1/T) \quad (4)$$

(The entropy was also obtained by integrating the heat capacity down in temperature, however, this method was found to be less efficient in that it required a finer grid of temperatures near the transition for equal accuracy).

The correlation functions Π_{MC} for a figure f were obtained by taking the thermal average (over the 10^6 Monte Carlo steps) of the product of Ising spin variables over the sites $1, 2, \dots, k_f$ of all symmetry-equivalent figures f [i.e., the thermal average of Eq. (1)].

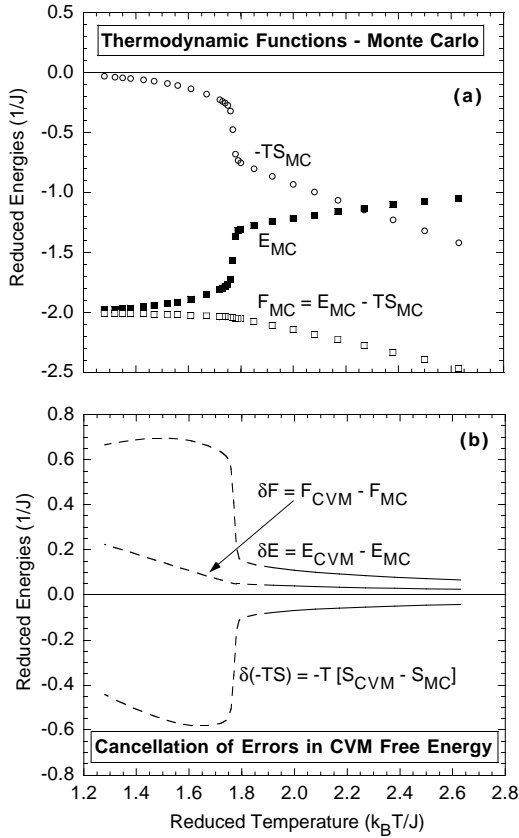


FIG. 1. Energy, entropy, and free energy as a function of temperature for the nearest-neighbor anti-ferromagnetic Ising model. All quantities are given in dimensionless units: $k_B T/J$ for temperature, energies are given normalized by J , and entropies are given normalized by k_B . (a) Results obtained from Monte Carlo simulations and thermodynamic integration. (b) Errors in standard CVM (disordered phase symmetry) compared to Monte Carlo. We have used only the CVM entropy expression with the disordered phase symmetry. Thus, in (b), differences with Monte Carlo for temperatures below the CVM transition ($T=1.89$) are overestimated and hence are shown as dashed lines (see text).

III. RESULTS

A. Analysis of CVM errors vis-a-vis MC simulations

The energy, entropy, and free energy obtained from Monte Carlo simulations are shown in Fig. 1a. The first-order transition at $T \simeq 1.77$ is evident from the discontinuity in energy and entropy. We have also computed the energy, entropy, and free energy predicted by CVM (in the tetrahedron approximation). By comparing these CVM results with the “exact” Monte Carlo results in Fig. 1a, we may ascertain the errors in thermodynamic functions of the CVM. The differences δE , $\delta(-TS)$, and δF between the respective CVM and Monte Carlo functions are shown in Fig. 1b. In our CVM calculations, we have used only the CVM entropy expression with the disordered phase symmetry. Thus, in Fig. 1b differences with

Monte Carlo for temperatures below the CVM transition ($T=1.89$) are shown as dashed lines. Obviously, practitioners of CVM would correctly impose a lower symmetry on the entropy expression below the transition to the ordered phase and would not use the disordered phase symmetry in this temperature range. The reason we use the CVM disordered phase symmetry down to low temperature is due to our wish to combine CVM methods with MC, which as we describe in the next section, is problematic when using ordered expressions for CVM entropy.

As indicated in the Introduction, the CVM correlation functions $\{\bar{\Pi}_f\}$ are closer to zero than the MC values. By Eq. (2), the CVM internal energy is less negative relative to Monte Carlo (thus, $\delta E > 0$ in Fig. 1b), demonstrating that the energetic effect of short-range order in CVM is underestimated, and hence the CVM internal energy is “more random” than that of Monte Carlo. The entropy of CVM is overestimated ($\delta(-TS) < 0$) relative to Monte Carlo, again indicating a more random solution than Monte Carlo. However, the error in the CVM free energy δF is simply the sum of the errors $\delta E + \delta(-TS)$. Since δE and $\delta(-TS)$ have opposite sign, they partially cancel, and give an error in free energy which is considerably smaller in magnitude than either the error in energy or in entropy. Thus, owing to the variational nature of the CVM,² the free energy of CVM is more accurate than one might expect from considering either the energy or entropy alone.

B. Using MC correlation functions in CVM calculations: Absence of cancellation of errors

Our foregoing discussion sheds light on a hybrid method which, naively thinking, might combine the accuracy of Monte Carlo with the simplicity of CVM. In this method, one uses the correlation functions $\{\bar{\Pi}_f\}$ (or equivalently, the cluster probabilities $\{\rho_j^f\}$) of MC simulations in the expressions for CVM entropy [Eq. (3)] and energy [Eq. (2)]. We refer to this method as the “ $F_{\text{CVM}}(\Pi_{\text{MC}})$ ” method. This method would, of course, require one to perform a Monte Carlo simulation for each composition and temperature of interest; however, one could, in principle, obtain the entropy at each point from a single Monte Carlo simulation (i.e., one composition and one temperature) rather than a series of Monte Carlo calculations which would be required for thermodynamic integration of the entropy. Since the Monte Carlo correlation functions are used in this method in Eq. (2), there is no error in energy ($\delta E = 0$). Thus, the error in free energy, shown in Fig. 2, is equal to the error in entropy: $\delta F = \delta(-TS)$. Since there is no error in energy in this method, there is no cancellation of errors. Hence, even though the exact Monte Carlo correlation functions are used in the “ $F_{\text{CVM}}(\Pi_{\text{MC}})$ ” method, it produces less accurate free energies than standard CVM: For example, at $T=1.92$, the free energies as given by Monte Carlo, “ $F_{\text{CVM}}(\Pi_{\text{MC}})$ ”, and CVM, are -2.109 , -2.050 , and -2.067 , respectively. (For comparison, CVM in the

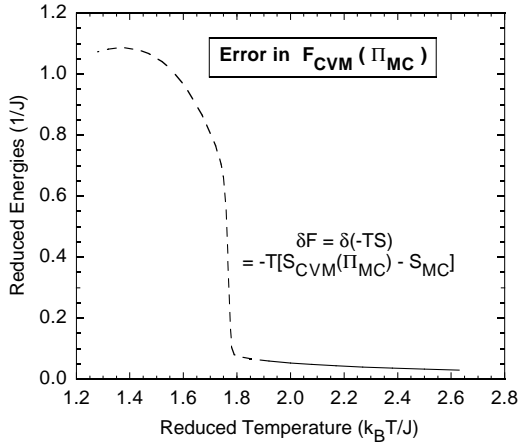


FIG. 2. Error in free energy as a function of temperature for the nearest-neighbor anti-ferromagnetic Ising model obtained using the “ $F_{CVM}(\Pi_{MC})$ ” method. All quantities are given in dimensionless units: $k_B T/J$ for temperature, energies are given normalized by J , and entropies are given normalized by k_B . In the “ $F_{CVM}(\Pi_{MC})$ ” method, MC correlation functions and cluster probabilities are used in the CVM expressions for energy and entropy, respectively. We have used only the CVM entropy expression with the disordered phase symmetry. Thus, differences with Monte Carlo for temperatures below the CVM transition ($T=1.89$) are overestimated and hence are shown as dashed lines (see text). Note that in this method, the energy is precisely that of Monte Carlo, thus the error in $-TS$ is also the error in free energy.

Tetrahedron-Octahedron approximation gives $F = -2.094$ for this temperature.)

Other disadvantages of the $F_{CVM}(\Pi_{MC})$ approach are illustrated in Fig. 3, showing a comparison of the entropies as a function of temperature as calculated by MC (S_{MC}), by standard CVM [$S_{CVM}(\Pi_{CVM})$], and by the $F_{CVM}(\Pi_{MC})$ method [$S_{CVM}(\Pi_{MC})$]. (The other two curves of Fig. 3 are discussed in Sections III C and III D below.) One can again see that (i) standard CVM (solid line) overestimates the entropy at high temperatures relative to Monte Carlo (open squares), (ii) the CVM entropy of the disordered phase is not applicable at low temperatures, and (iii) the $F_{CVM}(\Pi_{MC})$ method underestimates the entropy at high temperatures, and at low temperatures this entropy takes on the unphysical values $S_{CVM}(\Pi_{MC}) < 0$. These unphysical values are a result of the fact that the expression for the *disordered* S_{CVM} allows negative values for many atomic configurations. For instance, in the *fcc* lattice, the simplest ordered configurations such as $L1_0$, $L1_1$, $L1_2$ have negative S_{CVM} values. (These negative values of CVM entropy are likely to persist no matter what sized maximal cluster is used, and thus will always lead to difficulties with the $F_{CVM}(\Pi_{MC})$ method at lower temperatures, since the CVM entropy will incorrectly tend to negative values rather than zero.) Of course, one might argue that these ordered configurations only possess negative CVM entropy when evaluated with the CVM expression for the disordered phase, whereas when evaluated with the CVM expressions for

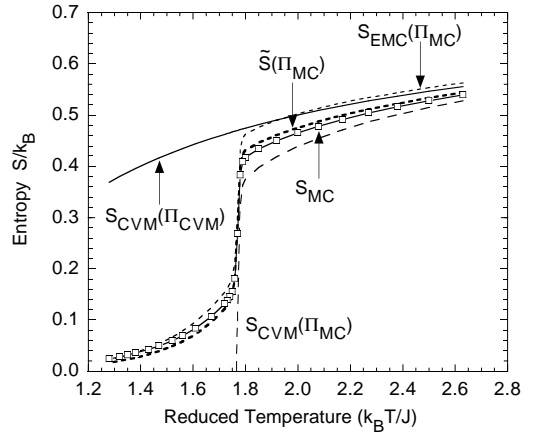


FIG. 3. Entropy versus temperature for the near-neighbor anti-ferromagnetic Ising model. The open squares (connected by a solid line) is the result of Monte Carlo simulations, the solid line is standard CVM, the long dashed line is the CVM entropy expression evaluated with the Monte Carlo cluster probabilities, the thin short dashed line is the result of the entropic Monte Carlo calculations, and the thick short dashed line is the simple correction to the CVM, the “modified CVM”.

the corresponding ordered phases, they will have non-negative entropies. However, this illuminates another potential problem with the $F_{CVM}(\Pi_{MC})$ method: In Monte Carlo simulations, the presence of anti-phase boundaries and finite-sized domains of long-range order preclude one from unambiguously defining the distinction between sublattices and extent of long-range order present in the simulation. However, an *ordered* CVM expression for the entropy is written in terms of correlation functions and cluster probabilities for all the symmetry-distinct figures for the symmetry of the long-range ordered phase. Thus, the CVM ordered entropy expressions presuppose the domains of long-range order are infinite in size, and hence the distinction of various sublattices in the ordered phase is unambiguous. Thus, using the “ $F_{CVM}(\Pi_{MC})$ ” method with ordered CVM entropy expressions is not practical because one doesn’t know from the MC simulations precisely how to divide the MC simulations into sublattices of long-range order and hence one does not even know from the MC simulations which ordered CVM expression to use. Also one does not know at what temperature to change the symmetry of the CVM to the ordered entropy expression. Thus, an ideal method combining Monte Carlo and CVM would only use a *single* expression (e.g., the disordered CVM expression) for the entropy at both low and high temperatures. We next describe such a method called “Entropic Monte Carlo” (EMC).

C. The entropic Monte Carlo method: A critical evaluation of CVM entropy

Lee⁷ has shown a practical way to determine the entropy of a Monte Carlo cell as a function of any state vari-

able. We call this method Entropic Monte Carlo (EMC). Though in his paper Lee applies the EMC method to the case of the energy as state variable in a quantized system, here we describe instead S_{EMC} in terms of the state variable $S_{\text{CVM}}(\sigma)$ which is a continuous, not quantized, variable. Our strategy will be to calculate $S_{\text{EMC}}(S_{\text{CVM}})$ by the method of Lee, and then insert $S_{\text{CVM}}(\Pi_{\text{MC}})$ into this expression, giving $S_{\text{EMC}}[S_{\text{CVM}}(\Pi_{\text{MC}})]$ which we write as $S_{\text{EMC}}(\Pi_{\text{MC}})$. We will show that this function reproduces very well S_{MC} . First, we describe how $S_{\text{EMC}}(S_{\text{CVM}})$ is calculated:

The EMC method is a self-consistent process in which each iteration is made from a series of Monte Carlo sweeps where the driving ‘‘energy’’ $E(\sigma)$ of the Monte Carlo equations is not the true energy contained in the sample but an approximation to the *entropy*:

$$E(\sigma) = E[S_{\text{CVM}}(\sigma)] \quad (5)$$

which depends on the configuration σ through the function $E[S_{\text{CVM}}]$, whose argument is the CVM entropy (per site) calculated with Eq.(3) for the cluster probabilities $\rho_j^f(\sigma)$ of the configuration σ . The function $E[S_{\text{CVM}}]$ is assumed to be monotonic. The EMC dynamics are given by the detailed balance condition

$$\exp[-E(\sigma_i)] W(i \rightarrow j) = \exp[-E(\sigma_j)] W(j \rightarrow i) \quad (6)$$

where W are transition rates and $E(\sigma)$ is given by Eq. (5). After many MC sweeps of the full lattice, one obtains a histogram

$$H(\bar{S}_{\text{CVM}}) = X d(\bar{S}_{\text{CVM}}) \exp[-E(\bar{S}_{\text{CVM}})] \quad (7)$$

where $d(\bar{S}_{\text{CVM}})$ is the number of configurations with a given value \bar{S}_{CVM} of the CVM entropy (degeneracy in S_{CVM}) and X is a constant of proportionality. We distinguish \bar{S}_{CVM} , which is a numerical argument attaining certain value, from S_{CVM} which is a function of both the microstate [through Eq.(3)] and the cluster probabilities $\rho_j^f(\sigma)$. The density of states function of the CVM entropy S_{CVM} is given by

$$\begin{aligned} D(\bar{S}_{\text{CVM}}) &= \sum_{\sigma} d(\bar{S}_{\text{CVM}}) \delta(\bar{S}_{\text{CVM}} - S_{\text{CVM}}(\sigma)) \\ &= (1/X) \sum_{\sigma} \exp(E(\bar{S}_{\text{CVM}})) H(\bar{S}_{\text{CVM}}) \times \\ &\quad \delta(\bar{S}_{\text{CVM}} - S_{\text{CVM}}(\sigma)) \end{aligned} \quad (8)$$

and the entropy $S_{\text{EMC}} = S(\bar{S}_{\text{CVM}})$ per site is defined as

$$\exp[NS(\bar{S}_{\text{CVM}})] = \int_{-\infty}^{\bar{S}_{\text{CVM}}} D(\xi) d\xi \quad (9)$$

where N is the number of sites in the MC cell.

From Eqs.(8) and Eq.(9), we may obtain the difference between the entropy at two different values \bar{S}_{CVM} .

$$S(\bar{S}_{\text{CVM}}^{(2)}) - S(\bar{S}_{\text{CVM}}^{(1)}) =$$

$$\begin{aligned} &\frac{1}{N} \ln \left[\sum_{\sigma, S_{\text{CVM}}(\sigma) < \bar{S}_{\text{CVM}}^{(2)}} \exp(NE[S_{\text{CVM}}(\sigma)]) \times \right. \\ &H[S_{\text{CVM}}(\sigma)] \\ &\left. - \frac{1}{N} \ln \left[\sum_{\sigma, S_{\text{CVM}}(\sigma) < \bar{S}_{\text{CVM}}^{(1)}} \exp(NE[S_{\text{CVM}}(\sigma)]) \times \right. \right. \\ &H[S_{\text{CVM}}(\sigma)] \end{aligned} \quad (10)$$

which is the basic equation used to determine the entropy from the EMC runs. On the right-hand side of Eq. (10), the sums are over the microstates σ obtained in the EMC sweeps whose CVM entropy $S_{\text{CVM}}(\sigma)$ are smaller than $\bar{S}_{\text{CVM}}^{(2)}$ or $\bar{S}_{\text{CVM}}^{(1)}$. As pointed out by Lee⁷, the entropy determination becomes especially simple when the interaction $E(S_{\text{CVM}})$ is such that the histogram $H[\bar{S}_{\text{CVM}}]$ is uniformly distributed and has little dependence on \bar{S}_{CVM} . In this case, Eq. (10) becomes

$$\begin{aligned} S(\bar{S}_{\text{CVM}}^{(2)}) - S(\bar{S}_{\text{CVM}}^{(1)}) &= \\ &\frac{1}{N} \ln \left[\sum_{\sigma, S_{\text{CVM}}(\sigma) < \bar{S}_{\text{CVM}}^{(2)}} \exp(NE[S_{\text{CVM}}(\sigma)]) \right] \\ &- \frac{1}{N} \ln \left[\sum_{\sigma, S_{\text{CVM}}(\sigma) < \bar{S}_{\text{CVM}}^{(1)}} \exp(NE[S_{\text{CVM}}(\sigma)]) \right]. \end{aligned} \quad (11)$$

Because of the factor of N , the exponential in Eq. (11) is a rapidly increasing function of S_{CVM} , and hence only the extremes contribute significantly to the sums, or

$$S(\bar{S}_{\text{CVM}}^{(2)}) - S(\bar{S}_{\text{CVM}}^{(1)}) \simeq \frac{1}{N} E(\bar{S}_{\text{CVM}}^{(2)}) - \frac{1}{N} E(\bar{S}_{\text{CVM}}^{(1)}) \quad (12)$$

This equation then suggests the self-consistent procedure for determining the entropy: From a crude estimate of $S(S_{\text{CVM}})$, we use Eq. (12) to obtain the interaction $E(S_{\text{CVM}})$ with which we make EMC runs, with which we recalculate $S(S_{\text{CVM}})$ from the basic Eq. (10). This process is taken to self-consistency. When self-consistency is reached, (i) the histogram $H[S_{\text{CVM}}]$ (the number of microstates in each small range of S_{CVM} obtained in a series of MC sweeps) is nearly constant, independent of the value of S_{CVM} and (ii) the driving ‘‘energy’’ which is the approximation to the entropy [Eq. (5)], becomes equal to the entropy calculated from the density of states [Eq. (9)], or in other words, the EMC entropy becomes exact. An important aspect of the EMC is that the calculated entropy functional form of $S(S_{\text{CVM}})$ *does not depend on any particular Ising Hamiltonian*, (so long as the important correlations are contained within the CVM maximal cluster), because the role of the ‘‘energy’’ driving the EMC calculations is played in Eq. (10) by the entropy itself.

Figure 4 shows a typical result $S_{\text{EMC}}(S_{\text{CVM}})$ of the EMC calculations, using a MC cell with $N = 12^3 = 1728$ sites. We also performed EMC calculations with different MC cells, with the results being slightly different for the larger negative values of S_{CVM} . The negative

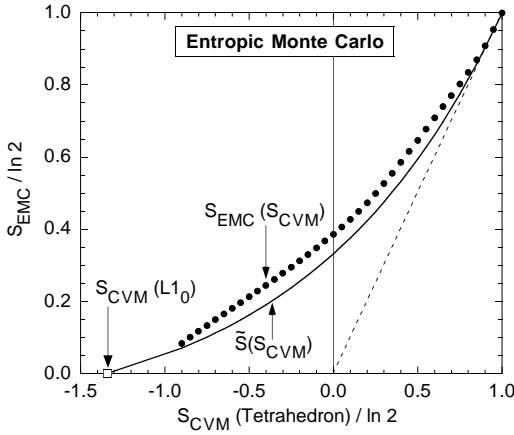


FIG. 4. Entropic Monte Carlo results for $S_{\text{EMC}} = S(S_{\text{CVM}})$. Filled circles are the EMC calculations, and the solid line is the EMC-inspired entropy functional $\tilde{S}(S_{\text{CVM}})$. The dashed line is line of unit slope simply to guide the eye. EMC was performed for a cell of $12^3=1728$ sites, using the CVM tetrahedron expression for the disordered entropy. Note that many configurations correspond to negative CVM entropy, with the most negative (for all configurations with ≤ 16 atoms per cell) being the $L1_0$ configuration.

values of S_{CVM} correspond to configurations of atoms with higher symmetry, usually associated with smaller repeat units, thus explaining why the curve depends to some extent on the size and shape of the MC cell for the negative values of S_{CVM} : For instance, for an EMC cell with an odd number of sites (e.g., 11^3), one could never obtain the stoichiometric configuration $L1_0$ with its large negative CVM entropy. In fact, simple high-symmetry configurations such as $L1_0$, $L1_1$, $L1_2$ all have negative values of S_{CVM} . Examining the CVM entropy for all configurations with up to 16 atoms per cell,¹⁰ we found the configurations with the most negative CVM entropy had very small unit cells. The largest negative CVM entropy occurs for $L1_0$ for which $S_{\text{CVM}}(L1_0) = -1.34 \ln 2$.

The results $S_{\text{EMC}}[S_{\text{CVM}}(\Pi_{\text{MC}})]$ of EMC are shown in Fig. 3, where they are contrasted with the results of Monte Carlo, CVM, and “ $F_{\text{CVM}}(\Pi_{\text{MC}})$ ”.¹¹ By comparing $S_{\text{EMC}}(\Pi_{\text{MC}})$ and $S_{\text{CVM}}(\Pi_{\text{CVM}})$ with S_{MC} , we see that the EMC and CVM entropies are equally accurate at high temperatures. Remarkably however, the EMC method also produces extremely accurate entropies at *low temperatures*, in qualitative contrast with the “ $F_{\text{CVM}}(\Pi_{\text{MC}})$ ” method. Thus, even though one only uses a single disordered expression for the CVM entropy in the EMC calculations, the EMC reproduces both high temperature (disordered) and low temperature (ordered) entropy values, with no need to change the CVM entropy expression at any point. Although the internal energy in EMC is exact (so this method does not benefit from the cancellation of errors noted in Sec. III A for the CVM), we see that EMC does not need to be correct due to *cancellation* of errors. Instead, it is accurate because its *individual terms*

(E and $-TS$) are accurate.

The EMC, like standard Monte Carlo, can be a computationally laborious procedure. However, our EMC calculations of $S(S_{\text{CVM}})$ suggest a very simple functional $\tilde{S}(S_{\text{CVM}})$ which is appealing because the correction *does not require one to perform an EMC calculation*. We next describe this simple correction.

D. An EMC-inspired new entropy functional

While $S_{\text{CVM}}(\Pi_{\text{MC}})$ can be inaccurate, $S_{\text{EMC}}[S_{\text{CVM}}(\Pi_{\text{MC}})]$ is accurate but computationally expensive. Thus we will now develop a new functional $\tilde{S}[S_{\text{CVM}}(\Pi_{\text{MC}})]$ which is both accurate and inexpensive.

The EMC results of Fig. 4 permit one to guess the behavior of the “exact” entropy $S(S_{\text{CVM}})$ (in the limit of $N \rightarrow \infty$) as a function of the CVM entropy obtained from a “good” maximal cluster (e.g., the tetrahedron or the tetrahedron-octahedron). This “true” entropy function $S(S_{\text{CVM}})$ should have the following properties:

(i) The most positive $S_{\text{CVM}}(x)$ entropy $S_{\text{CVM}}^{\text{MAX}}(x)$ should correspond to the exact entropy for this case, i.e., the ideal mixing entropy: $S(S_{\text{CVM}}^{\text{MAX}}) = S^0(x) = -k_B[x \ln x + (1-x) \ln(1-x)]$.

(ii) The slope of $S(S_{\text{CVM}})$ at the maximum value of $S_{\text{CVM}}^{\text{MAX}} = S^0$ should be unity because for nearly random configurations the CVM approaches the exact result: $\frac{dS}{dS_{\text{CVM}}}|_{S^0} = 1$.

(iii) The most negative value of the CVM entropy should correspond to zero “true” entropy. Thus, $S(S_{\text{CVM}}^{\text{MIN}}) = 0$. The configuration with most negative CVM entropy can be found by examining all configurations up to some maximum unit-cell size, as described in Ref. 10. For instance, for the tetrahedron CVM, $L1_0$ has the most negative CVM entropy [$S_{\text{CVM}}^{\text{MIN}} = S_{\text{CVM}}(L1_0) = -1.34 \ln 2$]. This point is indicated in Fig. 4 by a square.

(iv) The function $S(S_{\text{CVM}})$ should increase monotonically with S_{CVM} as one can see from Eq. (10). Also, $S(S_{\text{CVM}})$ has a positive curvature [due to the exponent of N in the right-hand side of Eq. (10)].

We select a simple functional form for $S(S_{\text{CVM}})$ which satisfies (i)-(iv) above (but otherwise possesses no special physical meaning.) However, use of this simple form will provide a means of evaluating energies and entropies which (a) is computationally much more efficient than either MC thermodynamic integration or EMC, (b) possesses MC accuracy, and (c) may be extended to use any maximal cluster of the CVM. The functional form we choose for the approximation $\tilde{S}(S_{\text{CVM}})$ to the true $S(S_{\text{CVM}})$ which satisfies the four properties (i)-(iv) above is:

$$\tilde{S}(S_{\text{CVM}}) = (S^0 - \frac{S^0}{\alpha}) + \frac{S^0}{\alpha} \exp[\alpha(\frac{S_{\text{CVM}}}{S^0} - 1)] \quad (13)$$

where α is the solution of

$$0 = (S^0 - \frac{S^0}{\alpha}) + \frac{S^0}{\alpha} \exp[\alpha(\frac{S_{\text{CVM}}^{\text{MIN}}}{S^0} - 1)]. \quad (14)$$

In the case of the tetrahedron CVM, $\alpha = 0.86917$. The function in Eq. (14) depends only on a single parameter S_{CVM}^{MIN} which can be easily estimated from an enumeration of small-unit-cell configurations¹⁰ *using any maximal cluster of the CVM method*. (In contrast, an EMC calculation as we described in Section III C is only practical for the tetrahedron CVM approximation.) While the negative S_{CVM} configurations, which correspond to highly symmetric arrangements of atoms, have no meaning in the standard CVM procedure (since in standard CVM one would use a different expression for CVM entropy to describe ordered phases), the main merit of a correction such as Eqs. (13)-(14) is to restore these highly ordered configurations into a single CVM expression by attributing a non-negative entropy to them. Naturally this correction, when used together with the Monte Carlo correlation functions, will be especially important near the transition when the ordered configurations begin to be important.

To test these ideas, we calculated $\tilde{S}[S_{CVM}(\Pi_{MC})] \equiv \tilde{S}(\Pi_{MC})$, where \tilde{S} is given by Eq. (13), and the CVM is executed within the tetrahedron approximation. One sees (Fig. 3) that this approach presents a remarkable improvement over the $F_{CVM}(\Pi_{MC})$ method in all temperature ranges, especially below the transition temperature where $S_{CVM}(\Pi_{MC})$ is negative. Also, the simple functional represented by $\tilde{S}(\Pi_{MC})$ effectively retains all of the improvements over $F_{CVM}(\Pi_{MC})$ that were obtained by the full EMC calculation. In fact, for high temperatures, the $\tilde{S}(S_{CVM})$ approach is even closer to the exact Monte Carlo results than the EMC calculations on which it was based! This fact can be understood by examining the EMC calculations in Fig. 4: Figure 4 shows that the EMC calculations using a cell of 1728 sites do not reproduce property (ii) above, $\frac{dS}{dS_{CVM}}|_{S^0} = 1$. In fact, the slope of the EMC curve in Fig. 4 is only about 0.82 at the maximum value of the entropy. EMC simulations with even smaller cells were typically found to possess even smaller slopes. Presumably, for larger EMC simulations one would approach the correct slope of unity. The slope of EMC being smaller than unity means that as one comes down from infinite temperature, or $S_{CVM} = \ln 2$, the EMC entropy maintains a larger value than it should. This explains why $S_{EMC} > S_{MC}$ for temperatures above the critical temperature. Because the $\tilde{S}(S_{CVM})$ approach was constructed to obey the requirement $\frac{dS}{dS_{CVM}}|_{S^0} = 1$, it corrects the error in the slope of EMC caused by the finite-sized simulation cell, and hence improves the entropy above the transition. The reason that the derivative of EMC is less than one for small cell sizes is due to the negative S_{CVM} configurations, which are typically high-symmetry, small-unit-cell configurations. Thus, these negative S_{CVM} states are represented more in small EMC cells relative to configurations with large-unit-cells and low symmetry. If the density of states in Eq. (9) becomes artificially large for the negative region of S_{CVM} (due to small EMC cells), it will have to be compensated by an artificially small density of states in the region of positive S_{CVM} [since

the integral in Eq. (9) is constrained by the fact that it must be 2^N at $S_{CVM} = \ln 2$.] Thus, the integral will grow more slowly than it should for CVM entropies approaching $\ln 2$, and hence the slope will be less than one.

IV. SUMMARY

The main accomplishment of this paper is to suggest a simple functional $\tilde{S}(S_{CVM})$ [Eqs. (13)-(14)] that improves the CVM entropy. The development was based on insights gained from our analysis of the CVM free energy (which showed cancellation of energetic *vs.* entropic errors), and from the EMC philosophy⁷ permitting one to express the true entropy as a functional of an approximate, but deterministic entropy. The new functional $\tilde{S}(S_{CVM})$ can be used in future applications either with CVM alone [simply by replacing the CVM entropy with Eq. (13) in any existing CVM program], or with a combination of CVM and Π_{MC} (using $\tilde{S}[S_{CVM}(\Pi_{MC})]$ as described in this paper).

Acknowledgements

LGF acknowledges support from NREL during his visit, where much of this work was carried out. Work at NREL was supported by the Office of Energy Research (OER) [Division of Materials Science of the Office of Basic Energy Sciences (BES)], U. S. Department of Energy, under contract No. DE-AC36-83CH10093.

-
- ¹ K. Binder, *Monte Carlo Methods in Statistical Physics: An Introduction*, Springer-Verlag, New York (1992); *Applications of the Monte Carlo Method in Statistical Physics*, edited by K. Binder, Springer-Verlag, New York (1987).
 - ² R. Kikuchi, Phys. Rev. **81**, 988 (1951); For a modern review, see e.g., D. de Fontaine, Solid State Phys. **47**, 33 (1994) or F. Ducastelle, *Order and Phase Stability in Alloys* (Elsevier, New York, 1991).
 - ³ Throughout this paper, all quantities are given in dimensionless units: $k_B T/J$ for temperature, energies are given normalized by J , and entropies are given normalized by k_B .
 - ⁴ See, for example, W. Schweika in *Structural and Phase Stability of Alloys*, edited by J. L. Moran Lopez, F. Mejia-Lira, and J. M. Sanchez, Plenum, New York (1992).
 - ⁵ These correlations are for a 16^3 Monte Carlo cell with 500 Monte Carlo steps (per site) discarded, and averages taken over the subsequent 30,000 steps.
 - ⁶ A.G. Schlijper and B. Smit, J. of Stat. Phys. **56**, 247 (1989).
 - ⁷ J. Lee, Phys. Rev. Letters **71**, 211 (1993).
 - ⁸ J. A. Barker, Proc. Roy. Soc. London **216**, 45 (1953).
 - ⁹ T. Morita, J. Phys. Soc. Japan **12**, 753 (1957).
 - ¹⁰ L.G. Ferreira, S.-H. Wei, and A. Zunger, Int. J. of Supercomputer Applications **5**, 34-56 (1991).

¹¹The results presented in Fig. 4 correspond to a grand canonical EMC for which the chemical potential, rather than composition x remained fixed. We also made canonical EMC runs by flipping pairs of opposite spins, thus maintaining constant x at the values 0.50 and 0.25. We obtain very similar results with either the canonical EMC or grand canonical EMC, provided that one normalizes both the EMC and CVM entropy with the ideal entropy, $-x \ln x - (1-x) \ln(1-x)$, instead of $\ln 2$ as in Fig. 4.